Electronic Supplementary Material (ESI) for Sustainable Energy & Fuels.

Supporting information

The climatic response of thermally integrated photovoltaic–electrolysis water splitting using Si and CIGS combined with acidic and alkaline electrolysis

İ. Bayrak Pehlivan[a], U. Malm[b], P. Neretnieks[b], A. Glüsen[c], M. Müller[c], K. Welter[c], S. Haas[c], S. Calnan[d], A. Canino[e], R. G. Milazzo [f], S. M. S. Privitera[f], S. A. Lombardo[f], L. Stolt[b], M. Edoff[a]*, and T. Edvinsson[a]*

[a] *Department of Engineering Sciences, Uppsala University, P.O. Box 534, 75121 Uppsala, Sweden*
[b] *Solibro Research AB, Vallvagen 5, Uppsala 75651, Sweden.*
[c] *Forschungszentrum Juelich GmbH, Wilhelm Johnen Strasse, Juelich 52428, Germany.*
[d] *PVcomB, Helmholtz-Zentrum Berlin für Materialien und Energie GmbH, Schwarzschildstrasse 3, Berlin 12489, Germany.*
[e] *ENEL Greenpower, Contrada Blocco Torrazze, Zona Industriale, Catania 95121, Italy.*
[f] *Consiglio Nazionale Delle Ricerche CNR-IMM, Zona Industriale, Ottava Strada, 5, Catania 95121, Italy.*

1. Experimental PV data

The Si cells utilized for the primary irradiance and temperature data in this project were commercial but the Si-modules were developed in the project. The CIGS PV cells and their modules were modified with higher Ga-content than conventional/commercial CIGS to match the demand of the alkaline catalyst system [1].

The experimental data of a 230 cm² SHJ mini–module consisting of three cells in series were provided at different temperatures between 25 and 80 °C. The efficiency dropped from 18.5 to 15.5 % (Fig. S1a) in the given temperature range. The data of a CIGS mini-module consisting of 118 cells in series were provided at different temperatures between 23 and 70 °C. A single cell area of the module was 54 cm^2. The efficiency for the given temperature range was between 17.4 and 14.4 % (Fig. S1b). The data of one solar cell based on PERT–Si with a cell area of 244 cm² were provided at different temperatures between 20 °C and 50 °C for an irradiance of 1000 W m^{-2}. The PV efficiency for the given temperature range was between 18.1 and 16.1 % (Fig. S1c). The experimental data of one TF–Si cell with a cell area of 1 cm² were provided at different temperatures between 25 and 80 °C. The efficiency for the given temperature range was between 11.5 and 9.9 % (Fig. S1d).

Table S1. Number of cells, active total area for the studied PV devices.

PV	**Number of cells**	**Active total area (cm²)**
SHJ	3	230
CIGS	118	6372
PERT-Si	1	243
TF-Si	1	1

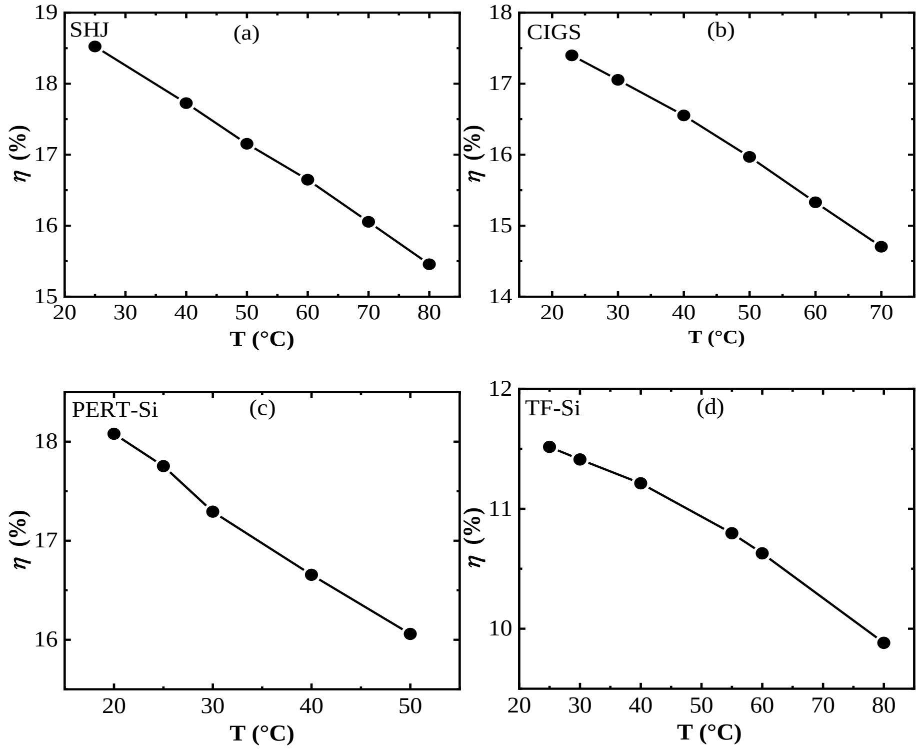

Figure S1. Temperature dependence of the cell efficiency obtained from experimental $j - V$ data (shown in Fig. 5) (symbols) at an irradiance of 1000 W m^{-2} for a (a) SHJ, (b) CIGS, (c) PERT-Si and (d) TF–Si cells.

2. Experimental electrolysis data

2.1 Pt (cathode) and IrO$_2$ (anode)

For the acidic electrolysis a CCM with an active area of 42*42 mm^2 based on Nafion 212 Membrane (thickness 51 μm) by Chemours was used. An anode loading of 2.35 mg/cm^2 IrO2 and a cathode loading of 0.81 mg of Pt was used. The MEA was made with Toray paper (TGP-H-120) as the porous transport layer on both sides as described previously [2]. A test cell with a serpentine flow field was used. The channel has a width and depth of 1.5 mm each and a total length of 55 cm. The lands between the channels have a width of 0.8 mm near the turn of the serpentine and 2.7 mm at the other end. Thus, the channel is slightly diagonal. Water was purified with a Millipore plant, preheated to the operating temperature and fed at a flow rate of 25 ml/min each into the anode and cathode channel. The cells were operated at ambient pressure. The experimental current-voltage data provided was for operation between 5 and 70 °C. The potential at 10 mA cm^{-2} at 25 °C was 1.51 V. 1-hour step ramping and 6-hour stability measurement were done with a laboratory built test-rig. The distance between anode and cathode was 0.005 cm.

2.2 NiMoW (cathode) and NiO (anode)

One of the alkaline electrolyzer consisted of NiMoW (cathode) and NiO (anode) having 1 cm^2 area and separated with an anion exchange membrane (Fumasep FAA-3-PK-130 Fuel Cell Store) in 1.0 M KOH. The electrocatalysts were prepared by coating the films on Ni foam substrates (thickness of 1.6 mm, the surface density of 350 g m^{-2}, and sheet resistance of 0.1 Ω/sq) using a Balzers UTT 400 reactive DC magnetron sputtering unit. The target was 5 cm diameter Ni, Mo, and W discs with 99.99% purity from Plasmaterials. The substrate holder was rotated at 3 rpm for the homogeneity of the films. Pre-sputtering was performed for 5 min to clean the surface of the targets. The Ar flow rate was 50 ml min^{-1}, and the total gas pressure was kept at 30 mTorr for all depositions. Sputter deposition at a power of 200 W was carried out for NiO anodic electrocatalysts with 10 % oxygen-to-argon ratio. The sputtering power of Ni, Mo and W targets were 80, 180, and 20 W for NiMoW cathodic electrocatalyst deposition, respectively. The film thicknesses on glass substrate determined by a Veeco Dektak 150 surface profilometry instrument were 165 ± 10 nm. 1-hour step ramping and 6-hour stability measurement were performed using 1 cm distance between the electrodes. A computer-controlled electrochemical workstation (BioLogic Science Instruments SP-200) was used for the measurements.

2.3 Pt-coated Ni foam (cathode) and Ni foam (anode)

The second alkaline electrolyzer consisted of a Pt-coated Ni foam (cathode) and Ni foam (anode) in 1.0 M KOH. The membrane was Zifron and the area of the catalysts were 4 cm^2. The polarisation curves were collected for an operating temperature range between 25 and 60°C. The potential at 10 mA cm^{-2} at 25°C was 1.52 V. 1-hour step ramping and 6-hour stability measurement were performed using 1 cm distance between the electrodes using a Keithley 2602 instrument. The catalysts with the area of 2 cm^2 were separated with the Zifron membrane and having zero gaps.

3. Equations used in the model

The maximum efficiency of PV modules was calculated by

$$\eta = j_{mp}\, V_{mp} \,/\, P_{Sun} \qquad (1)$$

where j_{mp} and V_{mp} are the current density and voltage at the maximum power point, respectively, and P_{Sun} is the solar irradiance.

The energy yield of the PV modules per active area was obtained from

$$E_{PV} = j_{mp} \times V_{mp} \times t \qquad (2)$$

where t is time.

The energy yield of the PV–electrolyzer devices normalized by the area is given by

$$E_{PV-C} = j_{op} \times 1.23 \times t \tag{3}$$

where j_{op} was the current density at the operation point, and 1.23 V is the minimum theoretical voltage to split water into hydrogen and oxygen (corresponding to a Gibbs free energy of 237.18 kJ per mol produced H_2 for the full water splitting reaction).

The share of electricity produced by the solar cells that are used for H_2 production, ETH, was obtained by

$$ETH = \frac{j_{op} \times 1.23}{j_{mp} \times V_{mp}} \eta_F \tag{4}$$

where η_F is the Faradic efficiency.

Solar–to–hydrogen efficiency of the PV–electrolyser systems was calculated from

$$STH = j_{op} \times 1.23 \; / \; P_{Sun} \tag{5}$$

The amount of H_2 produced by the PV–electrolysis systems was calculated from the duration and operation current. 1.0 A flow for 1 s produces 5.18 µmol H_2 which corresponds to 10.455 µg at standard temperature and pressure if there are no side reactions at the electrodes. The annually produced hydrogen was calculated as the sum of the hourly productions for an entire year.

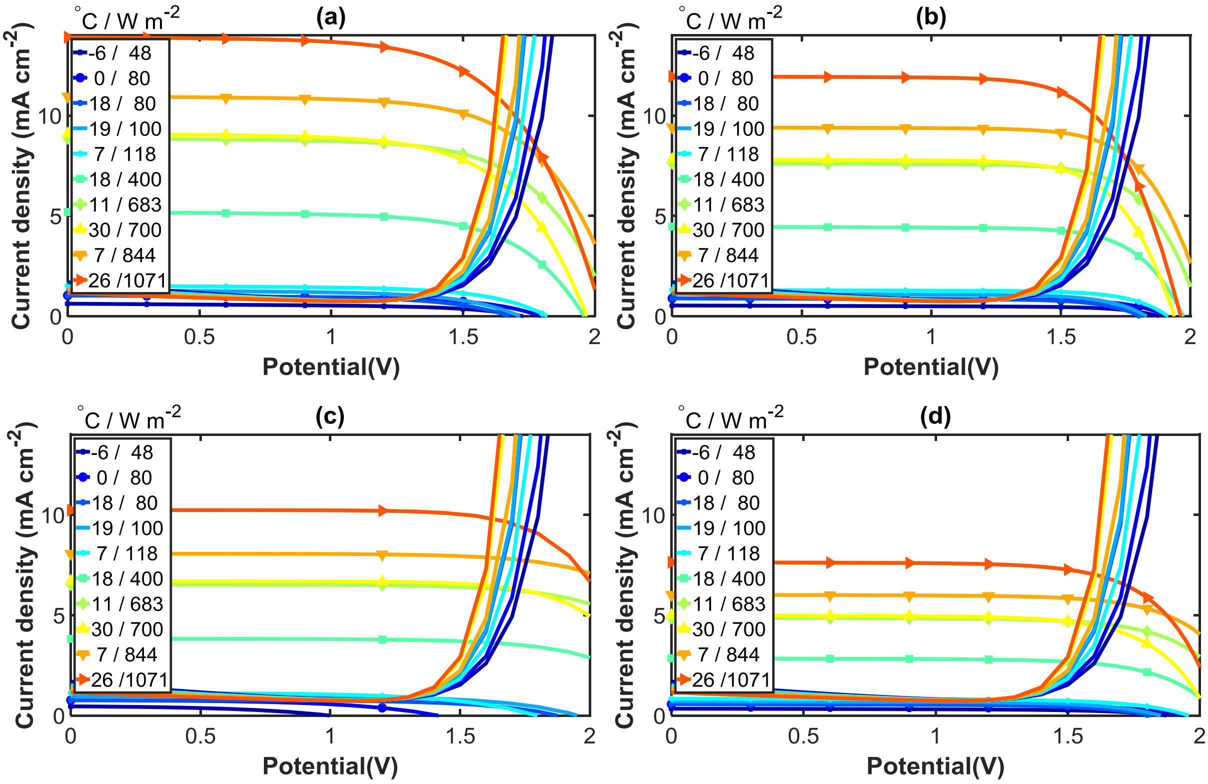

Figure S2. Exemplary $j-V$ data for Jülich climate with the same area of the alkaline NiMoW (cathode)-NiO (anode) electrolyser and PV approaches of (a) SHJ, (b) CIGS, (c) PERT–Si, and (d) TF–Si.

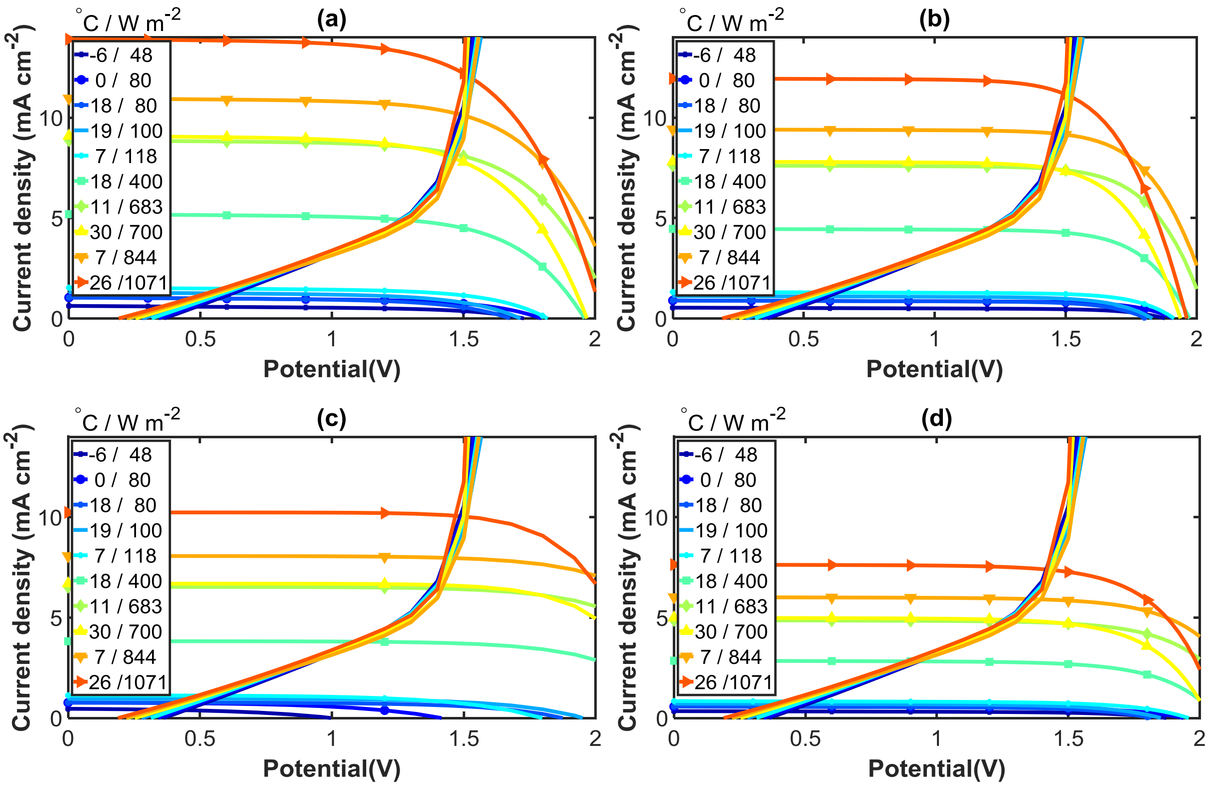

Figure S3. Exemplary $j - V$ data for Jülich climate with the same area of the alkaline Pt (cathode)-Ni foam (anode) electrolysis and PV approaches of (a) SHJ, (b) CIGS, (c) PERT–Si, and (d) TF–Si.

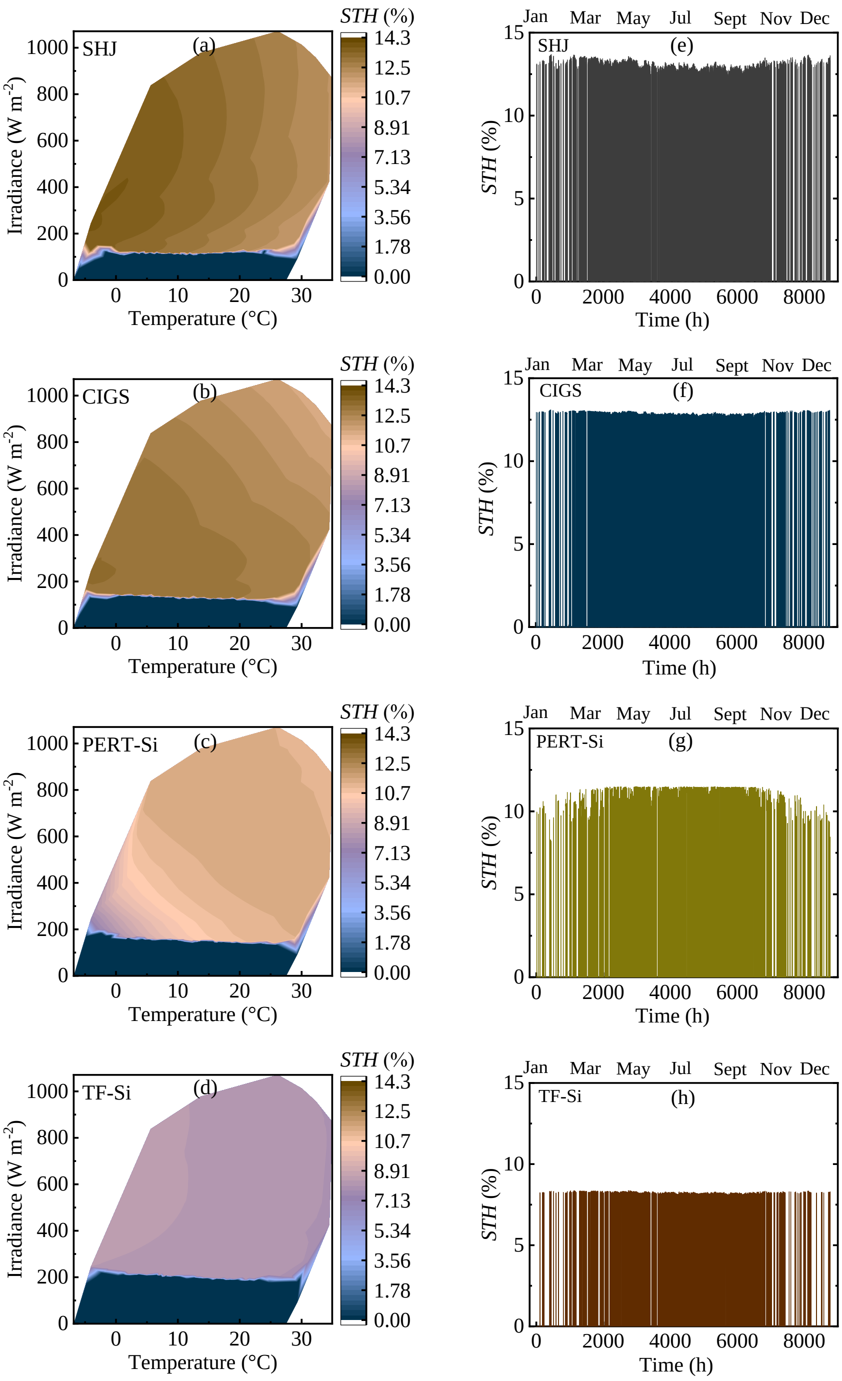

Figure S4. (a-d) Contour plot against irradiance and ambient temperature and (e-h) time distribution of *STH* efficiency in a year for all PV combined with NiMoW-NiO alkaline electrolysis with the same area (10 m^2) of the PV module and catalyst for Jülich climate with one-hour resolution.

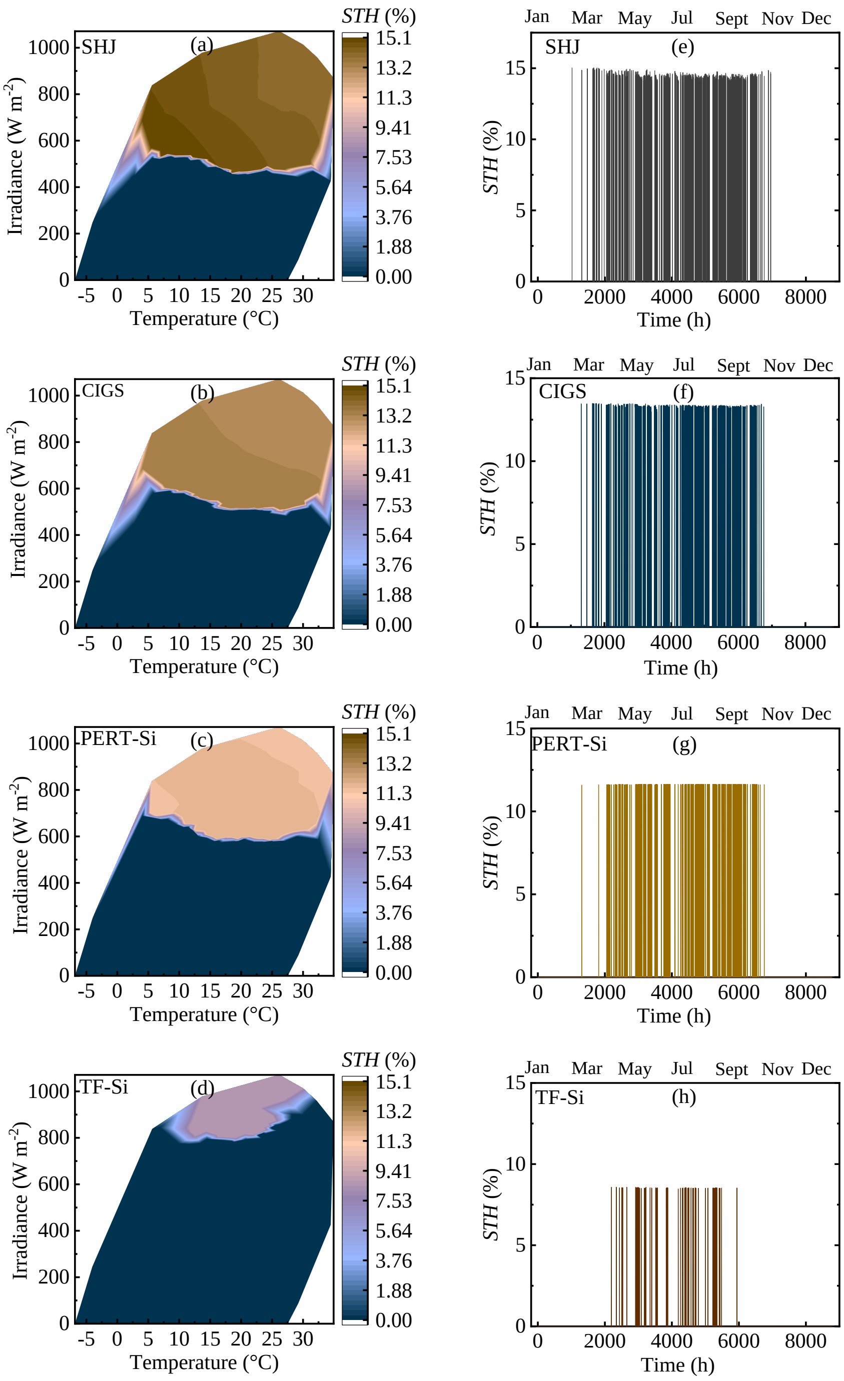

Figure S5. (a-d) Contour plot against irradiance and ambient temperature and (e-h) time distribution of *STH* efficiency in a year for all PV combined with Pt-Ni foam alkaline electrolysis with the same area (10 m^2) of the PV module and catalyst for Jülich climate with one hour resolution.

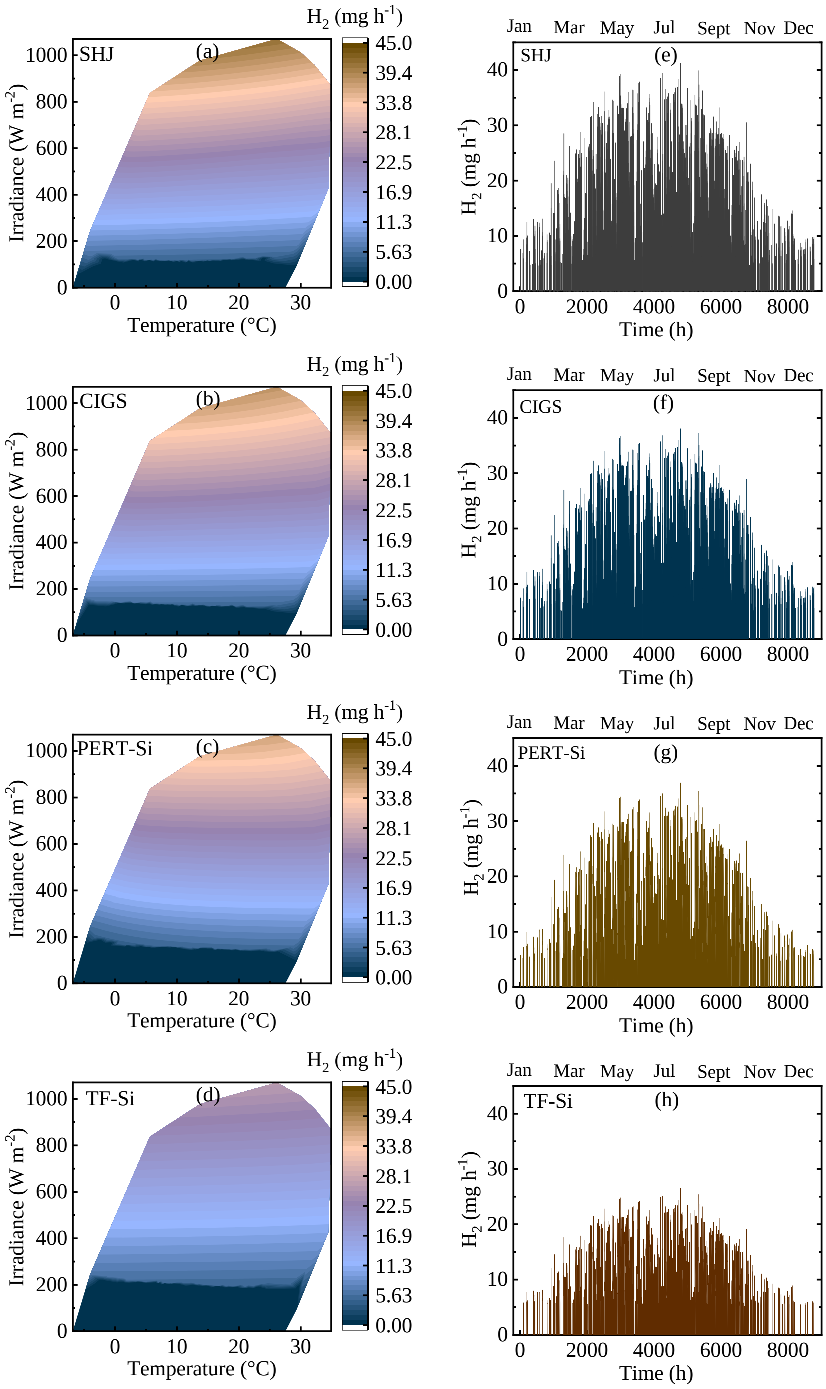

Figure S6. (a-d) Contour plot against irradiance and ambient temperature and (e-h) time distribution of H_2 production in a year for all PV combined with NiMoW-NiO alkaline electrolysis with the same area (10 m^2) of the PV module and catalyst for Jülich climate with one-hour resolution.

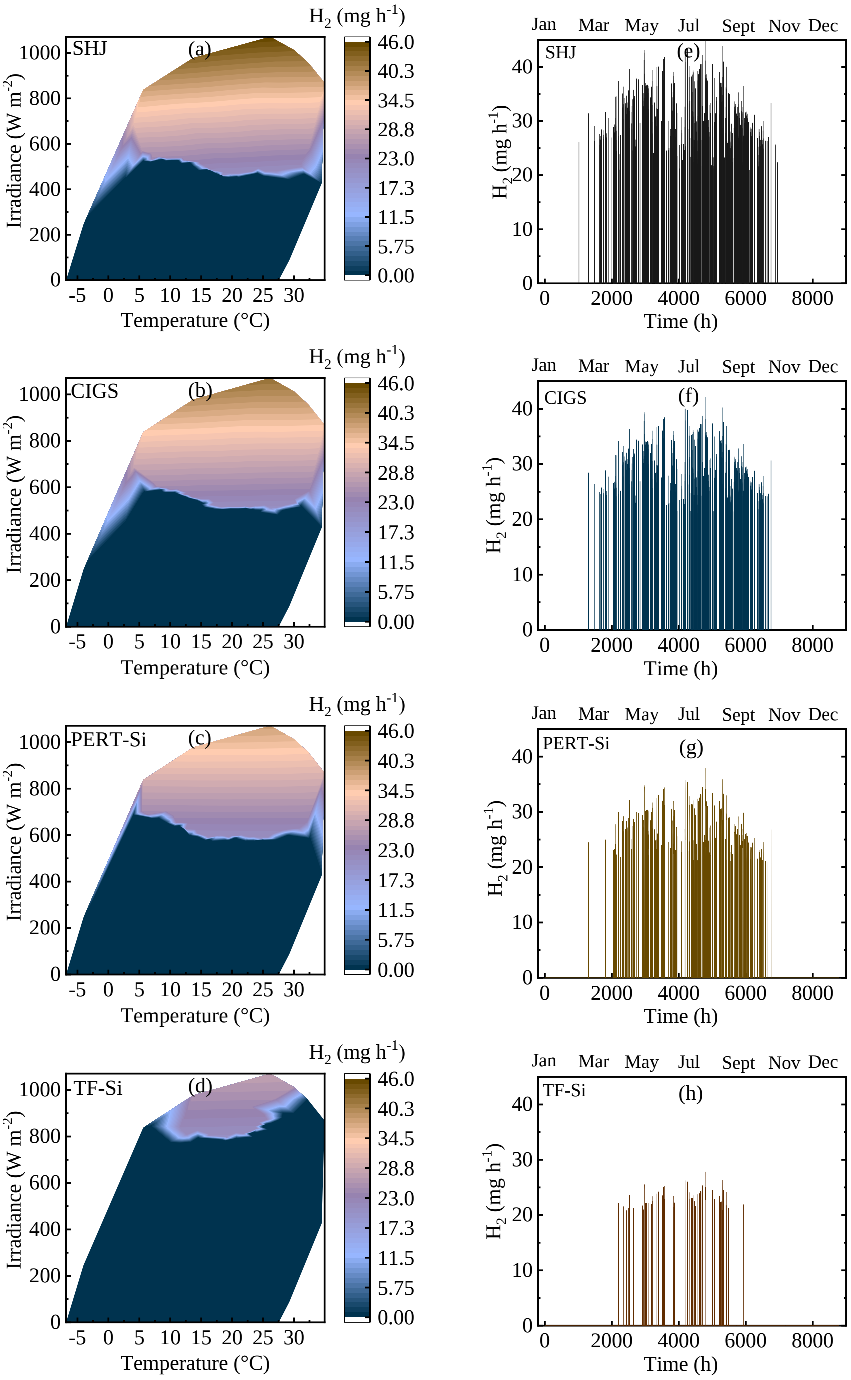

Figure S7. (a-d) Contour plot against irradiance and ambient temperature and (e-h) time distribution of H_2 production in a year for all PV combined with Pt-Ni foam alkaline electrolysis with the same area (10 m^2) of the PV module and catalyst for Jülich climate with one-hour resolution.

Table S2. Annual values of E_{PV-C}, ETH and STH efficiencies, yearly H_2 production from 1 cm^2 catalyst and for different catalyst areas combined with 10 m^2 PV for acidic Pt (cathode)-IrO_2 (anode) electrolysis.

SHJ	**A_C/A_{PV}**	**0.01**	**0.1**	**1**	**10**	**100**
	$E_{PV\text{-}C}$ (kWh m^{-2})	109	117	117	117	117
	ETH (%)	68	74	74	74	74
	STH (%)	11	12	12	12	12
	H_2 production from 1 cm^2 catalyst (mg h^{-1})	333	356	358	358	358
	H_2 production for 10 m^2 PV (kg $year^{-1}$)	33	36	36	36	36
CIGS	**A_C/A_{PV}**	0.01	0.1	1	10	100
	$E_{PV\text{-}C}$ (kWh m^{-2})	114	119	119	119	119
	ETH (%)	74	77	77	77	77
	STH (%)	12	12	12	12	12
	H_2 production from 1 cm^2 catalyst (mg h^{-1})	349	364	365	365	365
	H_2 production for 10 m^2 PV (kg $year^{-1}$)	35	36	36	36	37
PERT–Si	**A_C/A_{PV}**	**0.01**	**0.1**	**1**	**10**	**100**
	$E_{PV\text{-}C}$ (kWh m^{-2})	98	99	99	99	99
	ETH (%)	69	70	70	70	70
	STH (%)	10	10	10	10	10
	H_2 production from 1 cm^2 catalyst (mg h^{-1})	298	302	302	302	302
	H_2 production for 10 m^2 PV (kg $year^{-1}$)	30	30	30	30	30
TF–Si	**A_C/A_{PV}**	**0.01**	**0.1**	**1**	**10**	**100**
	$E_{PV\text{-}C}$ (kWh m^{-2})	74	75	75	75	75
	ETH (%)	75	76	76	76	76
	STH (%)	8	8	8	8	8
	H_2 production from 1 cm^2 catalyst (mg h^{-1})	225	229	229	229	229
	H_2 production for 10 m^2 PV (kg $year^{-1}$)	22	23	23	23	23

Table S3. Annual values of E_{PV-C}, ETH and STH efficiencies, yearly H_2 production from 1 cm^2 catalyst and for different catalyst areas combined with 10 m^2 PV for acidic NiMoW (cathode)-NiO (anode) electrolysis.

	A_C/A_{PV}	**0.01**	**0.1**	**1**
SHJ	$E_{PV\text{-}C}$ (kWh m^{-2})	27	79	116
	ETH (%)	17	50	73
	STH (%)	3	8	13
	H_2 production from 1 cm^2 catalyst (mg h^{-1})	82	241	352
	H_2 production for 10 m^2 PV (kg year^{-1})	8	24	35
CIGS	**A_C/A_{PV}**	**0.01**	**0.1**	**1**
	$E_{PV\text{-}C}$ (kWh m^{-2})	30	87.	110
	ETH (%)	19	56	71
	STH (%)	3	9	11
	H_2 production from 1 cm^2 catalyst (mg h^{-1})	92	267	336
	H_2 production for 10 m^2 PV (kg year^{-1})	9	27	34
PERT–Si	**A_C/A_{PV}**	**0.01**	**0.1**	**1**
	$E_{PV\text{-}C}$ (kWh m^{-2})	70	92	95
	ETH (%)	50	66	68
	STH (%)	7	10	10
	H_2 production from 1 cm^2 catalyst (mg h^{-1})	214	281	291
	H_2 production for 10 m^2 PV (kg year^{-1})	21	28	29
TF–Si	**A_C/A_{PV}**	**0.01**	**0.1**	**1**
	$E_{PV\text{-}C}$ (kWh m^{-2})	38	66	65
	ETH (%)	38	67	66
	STH (%)	4	7	7
	H_2 production from 1 cm^2 catalyst (mg h^{-1})	115	201	199
	H_2 production for 10 m^2 PV (kg year^{-1})	12	20	20

Table S4. Annual values of E_{PV-C}, ETH and STH efficiencies, yearly H_2 production from 1 cm^2 catalyst and for different catalyst areas combined with 10 m^2 PV for acidic Pt (cathode)-Ni foam (anode) electrolysis.

SHJ	**A_C/A_{PV}**	**0.01**	**0.1**	**1**
	$E_{PV\text{-}C}$ (kWh m^{-2})	72	114	143
	ETH (%)	45	71	90
	STH (%)	7	11	12
	H_2 production from 1 cm^2 catalyst (mg h^{-1})	219	335	201
	H_2 production for 10 m^2 PV (kg year^{-1})	22	33	20
CIGS	**A_C/A_{PV}**	**0.01**	**0.1**	**1**
	$E_{PV\text{-}C}$ (kWh m^{-2})	81	115	129
	ETH (%)	52	74	83
	STH (%)	8	12	12
	H_2 production from 1 cm^2 catalyst (mg h^{-1})	247	341	336
	H_2 production for 10 m^2 PV (kg year^{-1})	25	34	34
PERT–Si	**A_C/A_{PV}**	**0.01**	**0.1**	**1**
	$E_{PV\text{-}C}$ (kWh m^{-2})	89	103	112
	ETH (%)	63	73	80
	STH (%)	9	11	12
	H_2 production from 1 cm^2 catalyst (mg h^{-1})	271	300	291
	H_2 production for 10 m^2 PV (kg year^{-1})	27	30	29
TF–Si	**A_C/A_{PV}**	**0.01**	**0.1**	**1**
	$E_{PV\text{-}C}$ (kWh m^{-2})	63	76	83
	ETH (%)	64	77	84
	STH (%)	7	2	0
	H_2 production from 1 cm^2 catalyst (mg h^{-1})	192	218	18
	H_2 production for 10 m^2 PV (kg year^{-1})	19	22	2

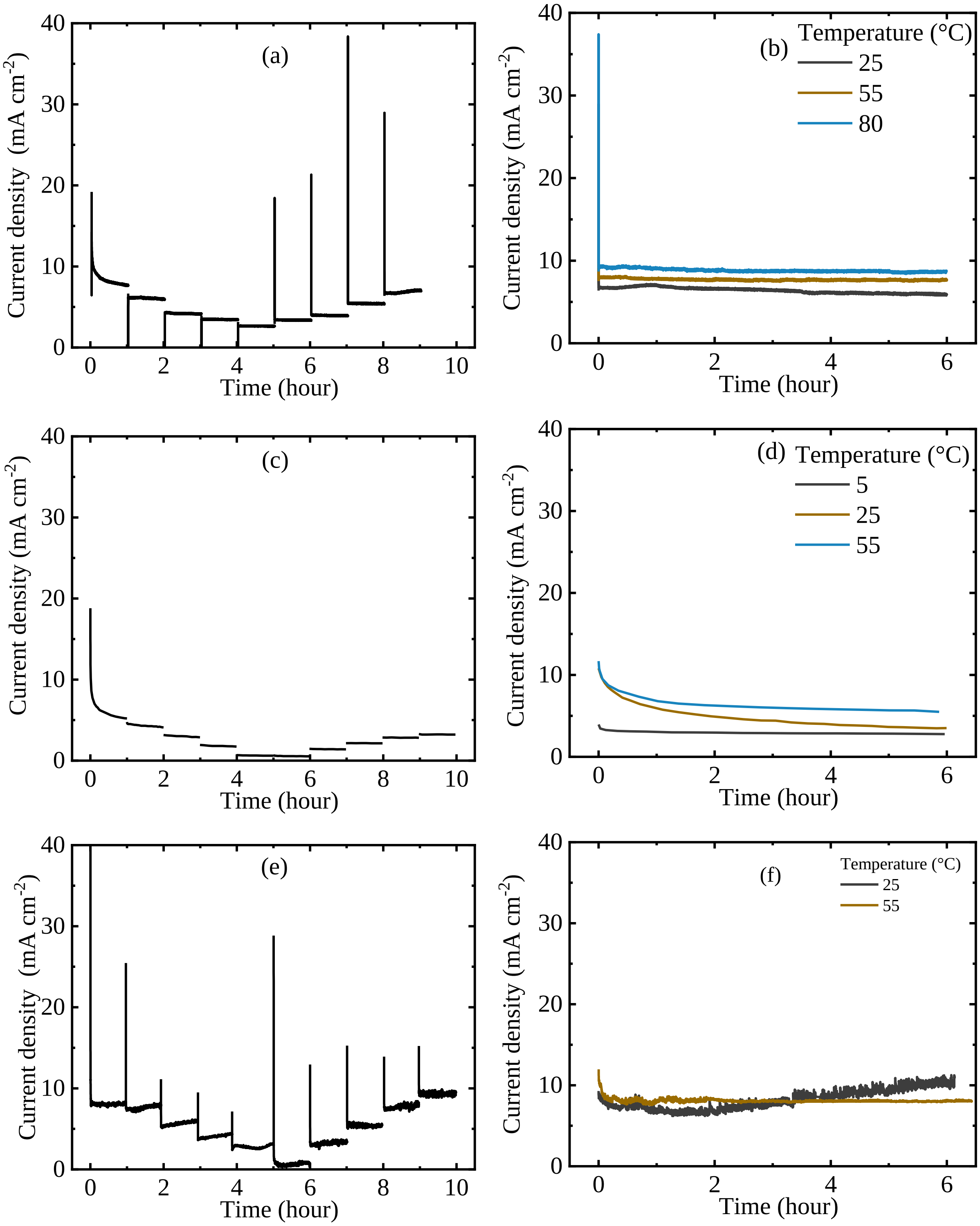

Figure S8. 1-hour step ramping at 25 °C and 6-hour stability measurement at different temperatures of (a-b) acidic Pt (cathode)-IrO_2 (anode), (c-d) alkaline NiMoW (cathode)-NiO (anode), and (e-f) alkaline Pt (cathode)-Ni foam (anode) electrolysis. 1-hour step ramping measurements were performed by applying potentials corresponding to 10, 8, 5, 3, and 1 mA cm^{-2}. The 6-hour stability measurement were performed at a potential which corresponds to 10 mA cm^{-2} in linear sweep measurements.

References

1. Bayrak Pehlivan, I., Edoff, M. Stolt, L. and Edvinsson, T. Energies, 2019, 12, 4064.
2. Müller, M., Carmo, M., Glüsen, A., Hehemann, M., Saba, S., Zwaygardt, W., Stolten, D., Water Management in Membrane Electrolysis and Options for Advanced Plants. Int. J. Hydrogen Energy 2019, 44, 10147-10155.